



Absorption in p-Ge QWs on Si. In: IEEE 13th International Conference on Group IV Photonics, Shanghai, China, 24-26 Aug 2016, pp. 30-31. ISBN 9781509019038 (doi:[10.1109/GROUP4.2016.7739130](https://doi.org/10.1109/GROUP4.2016.7739130))

This is the author's final accepted version.

There may be differences between this version and the published version. You are advised to consult the publisher's version if you wish to cite from it.

<http://eprints.gla.ac.uk/131481/>

Deposited on: 15 November 2016

Intersubband absorption in p-Ge QWs on Si

K. Gallacher,¹ A. Ballabio,² R. W. Millar,¹ J. Frigerio,² A. Bashir,³ I. MacLaren,³ Giovanni Isella,² Michele Ortolani,⁴ Douglas J. Paul¹

¹ University of Glasgow, School of Engineering, Rankine Building, Glasgow, G12 8LT, U.K.

² L-NESS, Dipartimento di Fisica del Politecnico di Milano, Como, 22100 Italy

³ University of Glasgow, School of Physics and Astronomy, Kelvin Building, Glasgow G12 8QQ, U.K.

⁴ Center for Life Nanosciences, Istituto Italiano di Tecnologia, Rome, 00185 Italy

Abstract— Mid-infrared intersubband absorption from p-Ge quantum wells with $\text{Si}_{0.5}\text{Ge}_{0.5}$ barriers grown on a Si substrate is demonstrated from 6 to 9 μm wavelength at room temperature and can be tuned by adjusting the quantum well thickness.

I. INTRODUCTION

There is an increased interest to develop Si based detectors that cover the important transmission windows within the mid-infrared (3-5 and 8-13 μm). Applications that could take advantage of this cheaper platform are biological and gas sensing spectroscopy [1]. SiGe quantum well (QW) infrared photodetectors have been previously demonstrated. However, these devices are limited to low detectivities due to the relatively large electron and hole effective masses and critical thickness limitations imposed by growth. Recently, intersubband absorption from p-Ge QWs has been experimentally demonstrated for the first time [2]. Ge QWs have the potential to improve performance significantly due to the lower effective masses and by allowing strain symmetrisation of the growth.

II. DESIGN AND MODELLING

The design consists of p-type compressively strained Ge QWs of either 5.4, 8.1, or 9.2 nm thickness, strain symmetrised with $\text{Si}_{0.5}\text{Ge}_{0.5}$ barriers. This allows the growth of a potentially unlimited number of periods without ever exceeding critical thickness limitations, thereby increasing overall absorption. Another benefit of p-Ge QWs is that it should provide larger absorption coefficients compared to p-SiGe designs, due to the smaller effective masses of the holes. In addition, by using the more complex non-parabolicity and strong coupling of the valence bands, this relaxes selection rules and allows both TE (x-y) and TM (z) polarization. Hence, both surface normal and waveguide geometry devices can be realized. The band energies and confined wavefunctions were calculated using a self-consistent 6-band $\mathbf{k}\cdot\mathbf{p}$ Poisson-Schrodinger solver. Figure 1 shows the calculated band structure for a 5.4 nm Ge QW and 3.6 nm $\text{Si}_{0.5}\text{Ge}_{0.5}$ barriers. It is clear that the ground state in the QW is HH1 due to strain splitting of the HH and LH bands. The HH2, LH1, and HH3, LH2 are at roughly the same energies within the QW.

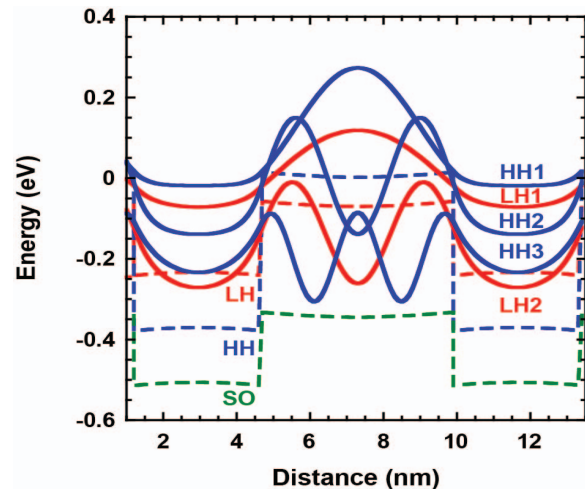


Figure 1. A schematic diagram of the calculated band structure for a 5.4 nm wide Ge quantum well sandwiched between 3.6 nm $\text{Si}_{0.5}\text{Ge}_{0.5}$ barriers.

III. GROWTH

The designed Ge QW structures were grown on a Si substrate by LEPECVD. A 600 nm linearly graded buffer from Si to $\text{Si}_{0.2}\text{Ge}_{0.8}$ was first grown, followed by a 400 nm p- $\text{Si}_{0.2}\text{Ge}_{0.8}$ bottom contact region ($N_A = 5 \times 10^{18} \text{ cm}^{-3}$). Then an undoped 10 nm $\text{Si}_{0.2}\text{Ge}_{0.8}$ spacer region was grown followed by the active region consisting of over 400 periods of either 5.4, 8.1, or 9.2 nm QWs sandwiched between $\text{Si}_{0.5}\text{Ge}_{0.5}$ barriers. Lastly, another undoped 10 nm $\text{Si}_{0.2}\text{Ge}_{0.8}$ spacer layer was grown, followed by a 20 nm p- $\text{Si}_{0.2}\text{Ge}_{0.8}$ top contact region. Graded buffer layers and the fully strained state of the superlattice were observed by x-ray diffraction (XRD) and Raman spectroscopy. Figure 2 shows the XRD spectra for the 8.1 nm QW structure. The Si(004) peak of the substrate is visible at $q = 7.365 \text{ nm}^{-1}$ and is used as a reference. Superlattice fringes are visible with a spacing that indicates a period of $\sim 12 \text{ nm}$. The zeroth-order fringe at 7.051 nm^{-1} is matched to the virtual substrate and indicates an average Ge content of 80% in the active layer stack. Raman spectroscopy was directly performed on the 8.1 nm QW sample by dry etching the cap and spacer region. With a pump at 532 nm wavelength this corresponds to a penetration depth of $\sim 20 \text{ nm}$, therefore it

should probe a full period of the active region. There is a convolution of the Ge-Ge phonon peak for the Ge QW and $\text{Si}_{0.5}\text{Ge}_{0.5}$ barriers and this is shown within the inset of Fig. 2. The Ge-Ge line of $\sim 302.7 \text{ cm}^{-1}$ for the QW indicates a compressive strain of $\sim 0.39 \%$.

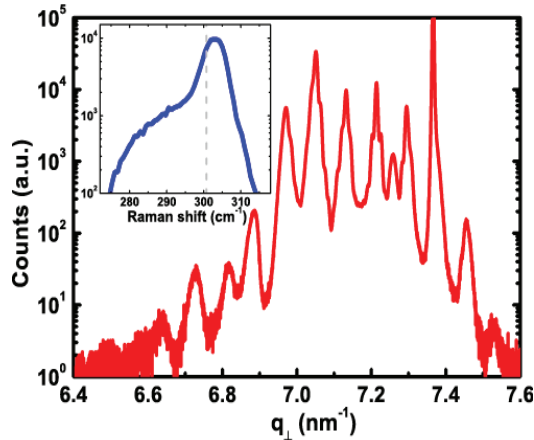


Figure 2. X-ray diffraction curves for the 8.1 nm wide Ge quantum well structure with 5.4 nm SiGe barriers grown on a Si substrate. The Inset shows the Raman spectrum for the 8.1 nm QW structure.

IV. CHARACTERISATION

Fourier transform infrared (FTIR) transmission measurements were performed on the as-grown 8.1 nm QW structure in vacuum at temperatures ranging from 6 to 300 K. The setup consisted of a Bruker IFS 66v interferometer and a nitrogen-cooled MCT detector. Blank chips were bonded onto the cold finger of an optical cryostat aligned within the sample chamber of the FTIR. Measurements were performed in surface normal (x-y) geometry with in-plane (TE) light polarization state defined by the properties of the Michelson interferometer. The electric field component parallel to the growth axis (TM) was null at all wavelengths before hitting the sample, but due to the refractive index variation of the complete structure there will be scattering that couples some radiation into TM polarized active transitions, so both TE and TM transitions will be observed. The normalized FTIR absorption spectra at 300 K in vacuum for the 8.1 nm QW structure is demonstrated in Figure 3 (a). The absorption peak at $\sim 0.17 \text{ eV}$ corresponds to the intersubband absorption. The QW design was for a bound-to-continuum transition from the HH2 to the mixed LH continuum formed from weakly / unconfined LH2 state that mixes with the HH3 bound state. The modelled absorption for an ideal TM and TE polarized light beam is also shown. The model agrees reasonably well with the experimental peak positions but at present underestimates the absorption width designs due the modelling not being able to account for broadening effects such as inhomogeneous broadening. The low temperature (6-200 K) absorption spectra of the 8.1 nm QW structure is demonstrated in Figure 3 (b). As the temperature decreases the intersubband absorption is increasing. There is a negligible intersubband

absorption temperature dependence observed. This arises from how both the band-edges of the barriers and QWs are changing at approximately the same rate in energy. It is also evident from there is a longer wavelength absorption peak appearing with decreasing temperature at $\sim 0.12 \text{ eV}$.

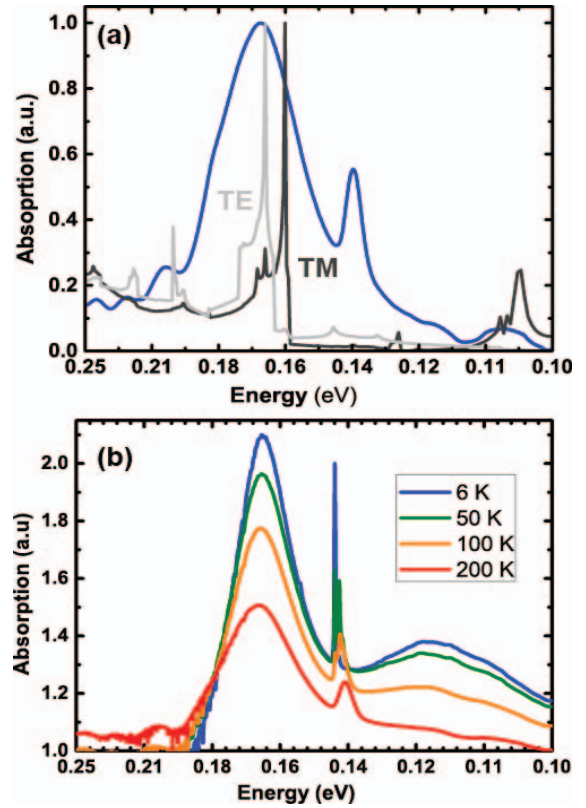


Figure 3. (a) Fourier transform infra-red (FTIR) absorption spectra at 300 K under vacuum for the as-grown 8.1 nm Ge quantum well (QW) structure. The modelled intersubband absorption spectra for TM and TE transitions is also displayed. (b) The low temperature FTIR absorption spectra of the 8.1 nm QW structure from 6-200 K.

V. CONCLUSION

Mid-infrared intersubband absorption of p-Ge QWs has been demonstrated. Band structure modelling has been undertaken and designs have been grown. High quality growth of the Ge QWs has been confirmed through XRD, Raman, and FTIR analysis. The modelled intersubband absorption agrees reasonably well with the experimentally observed intersubband absorption. It is envisaged that such designs could produce waveguide coupled photodetectors for spectroscopic sensing.

VI. REFERENCES

- [1] Baldassarre L., et al. "Mid-infrared plasmon-enhanced with germanium antennas on silicon substrates"; Nano Letters; 15 ,7225 (2015).
- [2] Gallacher, K., et al., Mid-infrared intersubband absorption from p-Ge quantum wells grown on Si substrates. Applied Physics Letters, 2016. 108(9). p. 091114.